Math. Struct. in Comp. Science (2007), *vol.* 17, *pp.* 225–246.
doi:10.1017/S0960129507005968 Printed in the United Kingdom

The driven three body Coulomb problem

JAVIER MADROÑERO[†‡], LAURENT HILICO[§], BENOÎT GRÉMAUD[§], DOMINIQUE DELANDE[§] and ANDREAS BUCHLEITNER[‡¶]

[†]*Physik Department, Technische Universität München, James-Franck-Straße, D-85747 Garching*
[‡]*Max-Planck-Institut für Physik komplexer Systeme, Nöthnitzer Str. 38, D-01187 Dresden*
[§]*Laboratoire Kastler Brossel de l'Université Pierre et Marie Curie et de l'Ecole Normale Supérieure, 4, place Jussieu, F-75252 Paris Cedex 05*
[¶]*Instytut Fizyki imienia Mariana Smoluchowskiego, Uniwersytet Jagielloński, Reymonta 4, PL-30-059 Kraków*

Received 15 May 2006; revised 6 October 2006

The three body Coulomb problem is one of the oldest unsolved problems of theoretical physics, and holds a variety of puzzling problems, on both the classical and quantum levels. It is of paradigmatic importance since it bears dynamical and spectral features that establish a link between single and many-particle dynamics, with the absolute minimum of ingredients. When additionally exposed to a time-periodic external perturbation, the effective dimension of the classical phase space as well as of Hilbert space increases dramatically. This gives rise to new phenomena, which stimulate research in such remote areas as mathematical physics, semiclassics and intense-field laser–matter interactions. In the present review, we illustrate how these different areas are interconnected by three interacting particles.

1. Introduction

At first glance, the Sun, Earth and Moon interacting through gravitational forces, and one nucleus and two electrons interacting through Coulomb forces, represent only minor variations on the gravitational Kepler problem and the hydrogen atom – in each case, only one particle has been added to the problem. Kepler motion and the hydrogen atom are perfectly well understood, and represent central chapters in any textbook on classical or quantum mechanics. Many particle dynamics is dealt with in condensed matter or nuclear physics, but three particles certainly are not 'many'. Yet, both the gravitational and the Coulomb three body problems are largely open issues as far as our theoretical and experimental understanding is concerned – our intention in this paper is to shed some light on the intricate dynamics of the three body Coulomb problem when exposed to an oscillating field.

1.1. *Classical and quantum features of three body dynamics*

The three body Coulomb problem is the microscopic version of the gravitational three body problem familiar from celestial mechanics, by which we imply that the substitution of gravitating masses by unequal and/or opposite charges does not change most of the

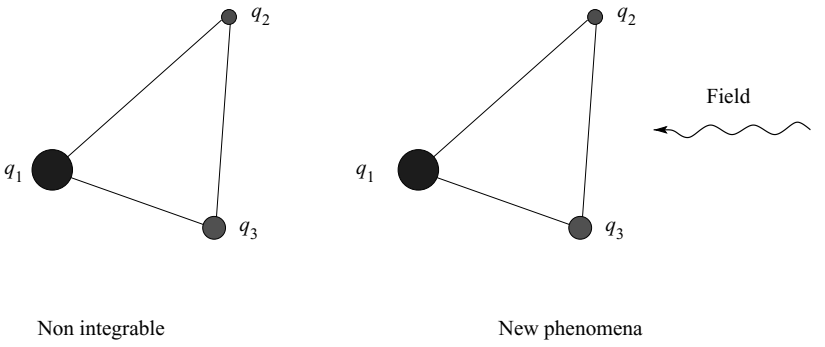

Fig. 1. The nonintegrable, unperturbed (left) and periodically driven (right) three body Coulomb problem. Under the external perturbation, energy is no more conserved, and different total angular momenta (composed from various combinations of the single electron angular momenta) are coupled. Consequently, the high dimensionality of the unperturbed problem is even enhanced – in classical phase space as well as in Hilbert space. A panoply of new physical phenomena is induced.

qualititative dynamical features. This configuration is naturally realised in the helium atom, and, to some extent, in the helium like alkali earths. If we consider both helium electrons independently, with both attracted by the doubly charged nucleus, we can think of each particle (in a semiclassical picture) moving on a Kepler like orbit, much as in the hydrogen atom. The (substantial) complication arises from the repulsive Coulomb interaction between the two electrons, which is long-range and singular, and can therefore mediate a very efficient energy exchange between the electrons. As a matter of fact, this electron–electron interaction renders the classical dynamics of the three body Coulomb problem nonintegrable, with a mixed, *regular-chaotic* phase-space structure (Richter *et al.* 1993). The classical nonintegrability was responsible for the failure of the early semiclassical formulation of quantum mechnics to explain the observed helium spectra (Tanner *et al.* 2000; Einstein 1917), and this was cured only in the early 1980's (Esra *et al.* 1991).

Let us also briefly consider the problem at the quantum level. Two independent electrons would give rise to two Rydberg series in the energy spectrum, with energies given by

$$E_{\text{indep}} = -\frac{2}{N^2} - \frac{2}{n^2}\,,\ N, n = 1, \ldots \infty\,, \tag{1}$$

and, in paricular, a ground state energy $E_{0,\text{indep}} = -4$ [a.u.]. The spectrum described by (1) is composed of a single electron Rydberg series $-2/n^2$, each of which converges, in the limit $n \to \infty$, to a single electron ionisation threshold at $-2/N^2$, for fixed, finite N. The single electron ionisation thresholds themselves converge towards the *double* ionisation threshold at energy $E = 0$, which is reached in the limit $N \to \infty$, $n \to \infty$. The single ionisation thresholds – accumulation points of the one electron Rydberg series – are also called 'single electron ionisation channels' and are labelled by the quantum number N of the second electron. The double ionisation threshold appears as an accumulation point of accumulation points, which implies a dramatic increase of the spectral density as we approach this limit.

https://doi.org/10.1017/S0960129507005968 Published online by Cambridge University Press

The electron–electron interaction now essentially shifts the ground state energy to $E_0 = -2.9037$ a.u., and couples the different N-channels. In particular, the bound states of the channels with $N > 1$ are coupled to the continuum states of the lower lying channels. This leads to a finite ionisation probability for doubly excited $(N, n > 1)$ electronic states of helium, and renders the *unperturbed* helium atom an open quantum system, with excited electronic states that exhibit a finite life time or decay rate. Formally speaking, this implies a strictly continuous, strongly structured spectrum above the first autoionisation channel $N = 1$. Note that the origin of the autoionisation on the quantum level is the same as the cause of the nonintegrability on the classical level: the Coulombic electron–electron repulsion!

1.2. *A paradigmatic, and minimalistic, case of complexity*

Hence, the helium atom comes up with the essential properties of a 'complex' quantum system:

— high spectral densities;
— strong coupling of the various (few) degrees of freedom;
— many-particle interactions;
— decay;

And all this with *minimal* ingredients: just three interacting particles. As we have already alluded to above, complex dynamics is not in general associated with apparently simple atoms, but rather with the typical objects of concern in solid state or nuclear systems – think, for example, of many particle dynamics in compound nuclear reactions (Figure 2) or, nowadays, of ultracold atoms in optical lattices (Figure 3), electronic transport in disordered solids (Kramer and MacKinnon 1993), or light scattering in random media (Wellens *et al.* 2005; Störzer *et al.* 2006).

In contrast with these 'obviously' complex systems, the Hamiltonian of the helium atom is perfectly well defined, and so is the cause of the complexity of its dynamics: the electron–electron interaction, which strongly couples the electronic degrees of freedom in a nonintegrable manner. Thus, helium establishes in many respects a paradigmatic link between single and many particle quantum dynamics, and we can expect that a rigorous understanding of this fundamental problem will have an important bearing for our understanding of the dynamics of strongly coupled multipartite quantum systems, which we are dealing with in such remote areas as photoinduced chemical reactions or large scale quantum computing. 'Rigorous' here implies that our aim must be a theory that offers predictive power and can be falsified by confronting its *quantitative* predictions with accurate experiments (which are becoming available now). Particularly in the realm of complex systems, such quantitative predictive power is crucial: complexity implies the competition of many physical processes at once. To predict such systems' behaviour, we ought to have a quantitative understanding of the relative weight of these processes under variable conditions. Such a programme requires the combination of various theoretical and numerical tools, from classical nonintegrable dynamics and semiclassical methods, through group theory to advanced parallel programming, and highlights the difference

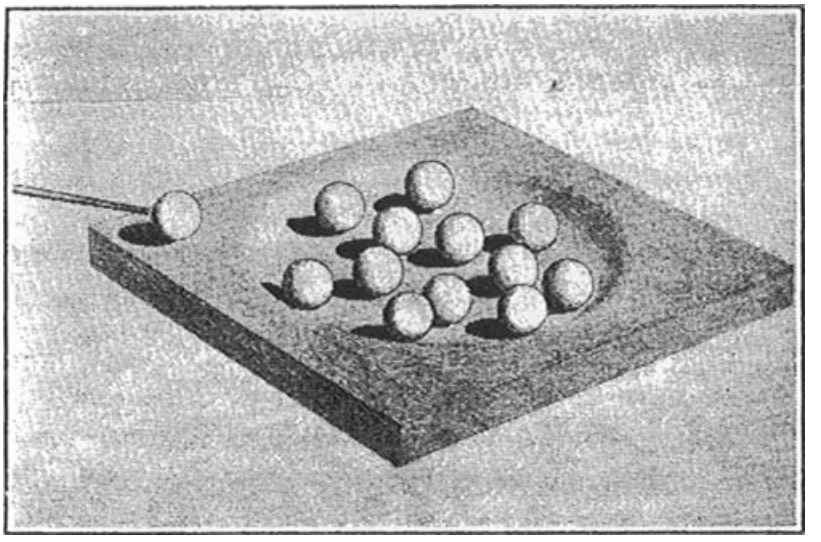

Fig. 2. Many-particle interactions then. A picture due to N. Bohr (Reprinted by Permission from Macmillan Publishers Ltd: Nature (Bohr 1936), copyright 1936), to sketch a compound nucleus reaction, where a neutron is injected into a heavy nucleus composed of weakly bound nucleons. Neither is the exact many particle Hamiltonian known here, nor can its various coupling constants be tuned. This motivated Wigner to formulate random matrix theory (Wigner 1959; Bohigas 1991) in order to describe the complicated scattering cross sections that are experimentally observed under such conditions (von Brentano *et al.* 1964).

between computational physics and computer games: the issue is *not to illustrate* a given set of experimental data by the simplest possible theoretical toy model, *but to guide* experiments in exploring the *terra incognita* of complex quantum dynamics with hard, quantitative theoretical predictions. This implies a long-lasting effort, where long distance runners' qualities are mandatory, but it promises to lead us to the solution of one of the last exactly (and this means: numerically exactly) solvable problems in quantum mechanics. When striving for this, we should remember a quote of Bertrand Russell in his 'ABC of Relativity' (Russell 1970): *The pursuit of quantitative precision is as arduous as it is important*.

2. Dynamics of driven helium

In our present contribution, we will focus on the dynamics of the *driven* three body Coulomb problem, which is realised experimentally by exposing helium or helium-like species to electromagnetic radiation. While the unperturbed three body dynamics already lives in a large, eight dimensional classical phase space, the time dependent external perturbation additionally destroys energy conservation and, in particular, couples different values of the total angular momentum (composed of the two electrons' individual angular momenta). At the classical level, this enlarges the phase space dimensions from eight

https://doi.org/10.1017/S0960129507005968 Published online by Cambridge University Press

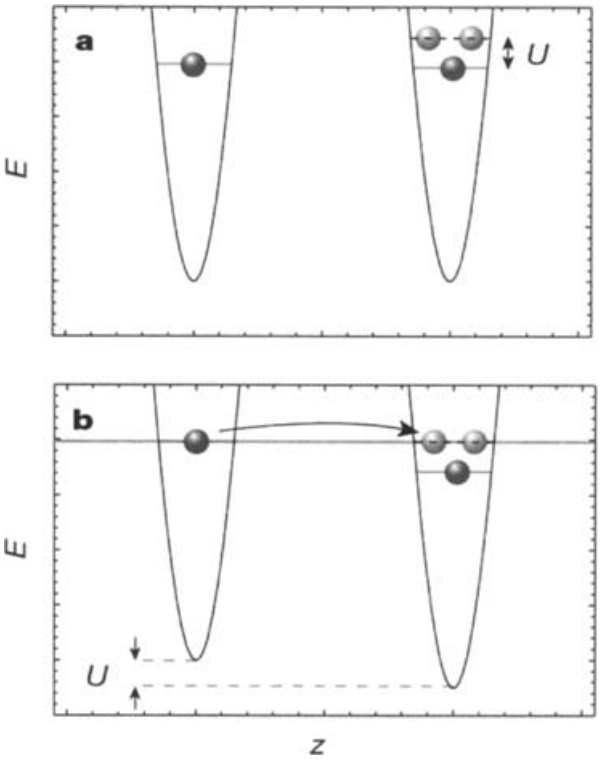

Fig. 3. Many-particle interactions now. In atomic physics and quantum optics labs, the control over composite quantum systems has reached unprecedented precision in recent decades. The plot (Reprinted by Permission of Macmillan Publishers Ltd: Nature (Greiner *et al.* 2002), copyright 2002) sketches two potential minima within a one dimensional optical lattice, where a controlled number of (ultra-) cold atoms are loaded. Not only is (or, at least, will be, in a very near future) the particle number perfectly controllable, but also the particle–particle interaction strength U can be tuned (top), and resonant tunnelling can be induced by a controlled tilt U of the lattice (bottom). This opens completely new avenues for our understanding of multiparticle quantum dynamics. The helium atom, possibly exposed to external fields, is the minimal version of a composite, multipartite quantum system, and is arguably the only really intermediate case between single and multiparticle dynamics.

to twelve. At the quantum level, it leads to a dramatic increase in the dimension of Hilbert space: the smaller the driving field frequency with respect to the (single or double) ionisation potential of the field free atomic initial state $|\psi_0\rangle$, and the higher the spectral density in the vicinity of $|\psi_0\rangle$, the larger the dimension. Furthermore, the external driving also induces a non-vanishing continuum coupling of the discrete eigenstates of the unperturbed atom, and thus renders the quantum spectrum strictly continuous. Consequently, the very size of the Hilbert space explored during the excitation and ionisation process of helium under external driving has so far hampered an accurate and complete analysis and understanding.

https://doi.org/10.1017/S0960129507005968 Published online by Cambridge University Press

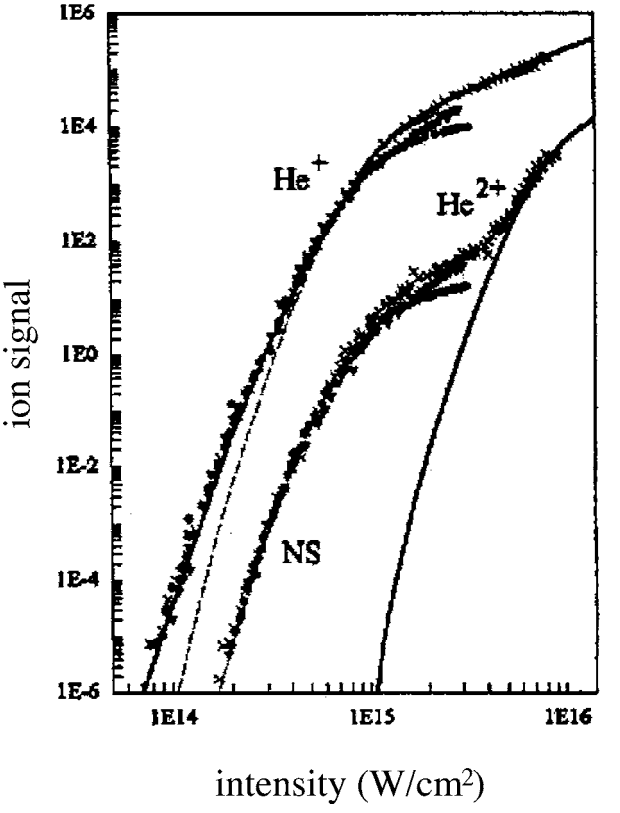

Fig. 4. Single and double ionisation yields of ground state helium under intense field driving. The symbols represent experimental data, while the dashed and continuous lines indicate the yields expected from an independent electrons picture (Walker *et al.* 1994) (courtesy of Louis DiMauro).

2.1. *Double ionisation from the atomic ground state*

Most of the experimental activity to date has focussed on the single and double ionisation of helium or similar species from the atomic ground state. In such experiments, the atoms are exposed to a short (in the femto-second range), intense laser pulse, and the relative abundance of singly and doubly charged ions after the laser–matter interaction is plotted on a double logarithmic plot as a function of the pulse's peak intensity – see Figure 4. The hallmark of the electron–electron interaction is the 'knee' structure observed in the double ionisation signal in these experiments: within a wide interval of field intensities, which spans approximately one order of magnitude, the experimentally observed double ionisation yield is several orders of magnitude larger than one would expect from an independent electron picture, which neglects the electron–electron interaction term in the Hamiltonian. This observation triggered extensive theoretical activities, generating a large number of model descriptions (Corkum 1993; Lappas *et al.* 1996; Lein *et al.* 2000) in order to grasp the qualitative features of the physical process underlying the experimentally observed ionisation signal. Since the driving field frequency $\omega/2\pi \simeq 780$ nm was rather

https://doi.org/10.1017/S0960129507005968 Published online by Cambridge University Press

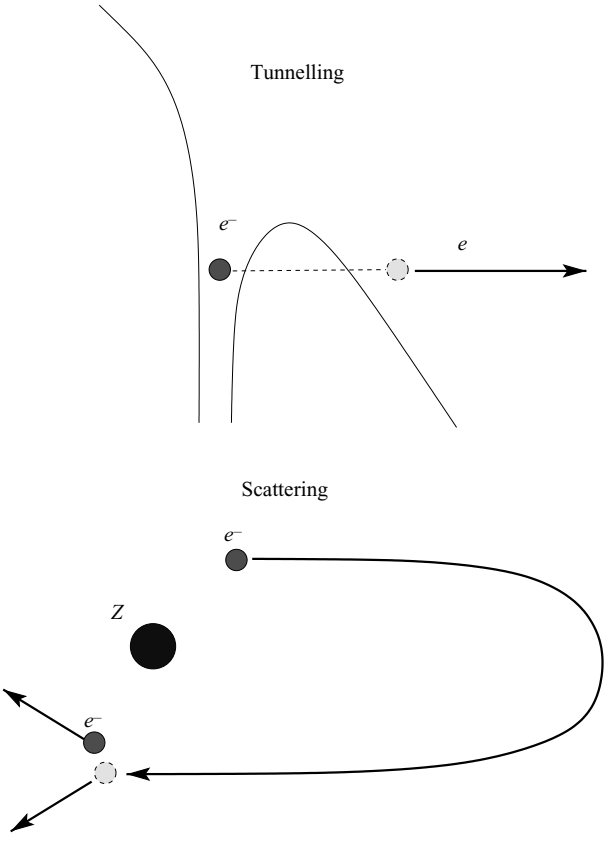

Fig. 5. The rescattering model (Corkum 1993). Under the external drive, one of two electrons is first set free from the attractive nuclear potential by tunnelling through the potential well created by the superposition of the driving field and Coulomb force, at a given phase ωt of the drive (top). The liberated electron then moves like a free charge in the oscillating field, with a maximal excursion of approximately $F/4\omega^2$ a.u., until the driving field changes its sign. Then the electron is accelerated backwards, towards the mother ion it left behind, and eventually knocks out the second electron, during the rescattering event (bottom). Whilst appealing and of stunning simplicity, this model is unable to provide a quantitative understanding of the double ionisation of helium by intense laser pulses from the ground state, and neglects any excitation processes into singly and doubly excited Rydberg states.

low in these experiments, requiring the absorption of approximately 50 photons to reach the double ionisation channel from the atomic ground state, a free electron would perform harmonic oscillations along the driving field's polarisation direction, with an amplitude that is large compared to the typical diameter of the atomic ground state. Thus, the most popular model to explain the observed double ionisation signal (Figure 5) assumes that one of the two ground state electrons is first set free from the nucleus' attractive potential by quantum tunnelling, then performs a full oscillation in the time periodic potential created by the driving field, and subsequently rescatters from the mother ion, thereby ejecting the second electron (Corkum 1993). Notwithstanding its appealing simplicity,

https://doi.org/10.1017/S0960129507005968 Published online by Cambridge University Press

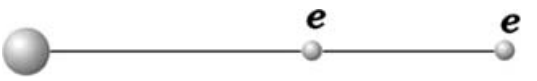

Fig. 6. Sketch of the classical frozen planet configuration (Richter and Wintgen 1990), which is a *stable* configuration of the unperturbed, classical three body Coulomb dynamics. Both electrons are located on the *same* side of the nucleus. In the collinear configuration shown, the outer electron is standing still at a fixed point in space, while the inner electron performs rapid oscillations along an extremal parabolic orbit of eccentricity one. The configuration is the result of a dynamical stabilisation phenomenon, which emerges from the competition of the various Coulomb interaction terms in the helium Hamiltonian.

this rescattering model obviously completely neglects the spectral (quantum) features of the physical system under study, and essentially builds on classical kinematics, amended by an initial tunnelling process that releases one electron from the Coulomb attraction by the nucleus. In particular, field induced excitation processes into the singly or doubly excited spectral range are not incorporated in the rescattering scenario. Therefore, no quantitative predictive power can be expected from such an approach, and the qualitative picture is bound to remain at a very crude level. In order to improve on this, a fully fledged quantum treatment including the singly and doubly excited spectral range will be needed, with the potential to guide more refined experiments that can assess more distinctive experimental observables than a simple ionisation signal. Note that partial progress has already been achieved in this direction (Scrinzi and Piraux 1997; Parker *et al.* 2000; Nikolopoulos and Lambropoulos 2001; Ruiz *et al.* 2006), but a theoretical and numerical approach valid in the full parameter range of non-relativistic atom–field interaction remains to be formulated. This will be our main concern later in this paper.

2.2. *The planar frozen planet state under external driving*

In our own theoretical treatment, we focus on the dynamics of a well-defined, highly correlated, doubly excited electronic state of the helium atom – the 'frozen planet' (Figure 6). From a theoretical point of view, this has the conceptual advantage that we start out from a classically and quantum mechanically well-characterised initial state that owes its very existence to a phase locking phenomenon between the motions of the inner and outer electrons (Richter and Wintgen 1990; Buchleitner *et al.* 2002). Indeed, as a consequence of the separation of time scales of the inner and outer electrons' dynamics, and of the interplay between electron–electron repulsion when both electrons come close to each other, and the attraction of the outer electron by the (screened, by the inner electron) nuclear charge when both electrons are far from each other, the outer electron experiences an effective, weakly binding potential sketched in Figure 7. The phase space structure associated with the outer electron's dynamics in this effective potential is illustrated by the Poincaré surfaces of section in Figure 8, in the absence and in the presence of the external drive. Clearly, the stability of the configuration against perturbations is spelled out by concentric, smooth, one dimensional manifolds, which express the existence of a local adiabatic invariant (Lichtenberg and Lieberman 1983), that is, of an approximate integral of motion. The frozen planet is anchored to this concentric structure, which is known as

https://doi.org/10.1017/S0960129507005968 Published online by Cambridge University Press

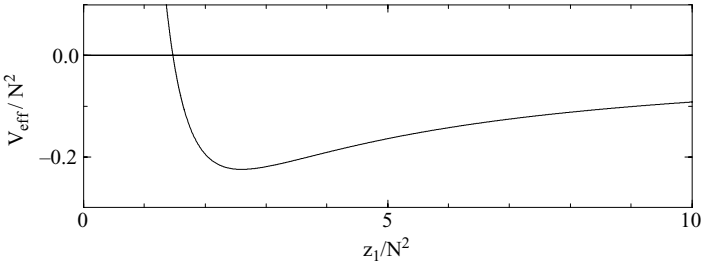

Fig. 7. Effective potential binding the outer electron in the frozen planet configuration (Ostrovsky and Prudov 1995), in units that are rescaled as a function of the excitation N of the inner electron. The potential can be deduced from the original Hamiltonian by averaging over the rapid motion of the inner electron. When the inner electron is at the outer turning point of its eccentric Kepler orbit, the interelectronic repulsion dominates, and the outer electron feels a net repulsive force. When the inner electron reaches its inner turning point, the outer electron experiences a net attractive force from the screened nuclear potential. On average, this generates a stable equlibrium point at a certain distance from the nucleus, given by the minimum of the effective potential.

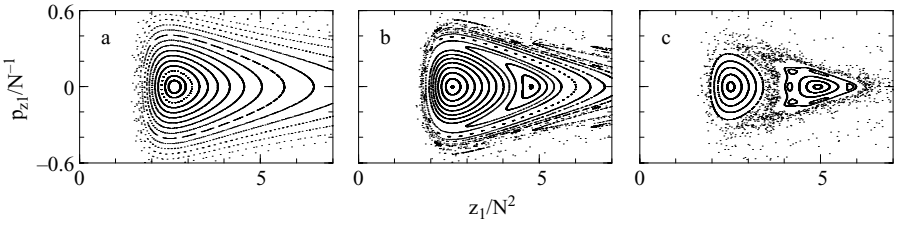

Fig. 8. Phase space structure of the outer electron of the frozen planet configuration, spanned by the electron's momentum p_{z1} and position z_1 along the configuration's symmetry axis, in units that are rescaled as a function of the excitation N of the inner electron.

a *nonlinear resonance* in the terminology of nonlinear classical mechanics (Chirikov 1959; Lichtenberg and Lieberman 1983; Buchleitner *et al.* 2002). Furthermore, we also see that, in the presence of the external perturbation, chaos invades phase space, at the expense of the original resonance island. However, a *second* resonance island is induced by the nonlinear coupling between the external field and the electronic degree of freedom, and its location in phase space depends on the choice of the frequency of the external drive (Schlagheck and Buchleitner 2003): the centre of the induced island will be located on that unperturbed periodic orbit that has an unperturbed oscillation frequency Ω (in the binding potential depicted in Figure 7) that is resonantly driven by the external frequency ω, that is, $m\Omega = \omega$, with integer m.

2.2.1. *Quantum-classical correspondence for the unperturbed frozen planet* Finally, we now aim to give a faithful quantum mechanical description of the driven frozen planet dynamics. However, we will be forced to content ourselves with a description that confines the three interacting particles to a plane that also comprises the field polarisation axis, simply due to the still limited capacity of currently available supercomputers. To get some

https://doi.org/10.1017/S0960129507005968 Published online by Cambridge University Press

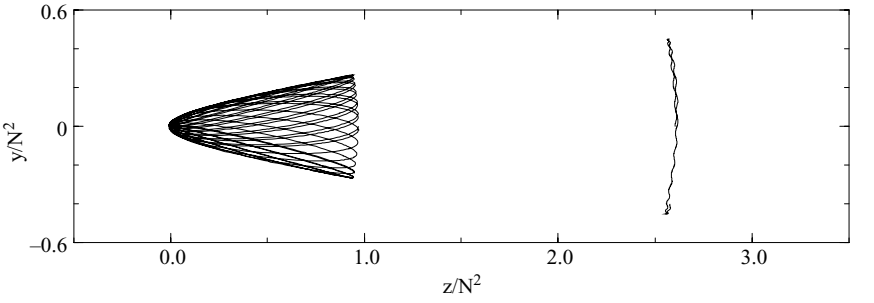

Fig. 9. Typical classical frozen planet trajectory, with a slight excitation in the plane transverse to the collinearity axis. While the inner electron precesses on a parabolic orbit, the outer electron remains perfectly correlated (transversally as well as longitudinally) with the inner electron's motion (Schlagheck and Buchleitner 2003).

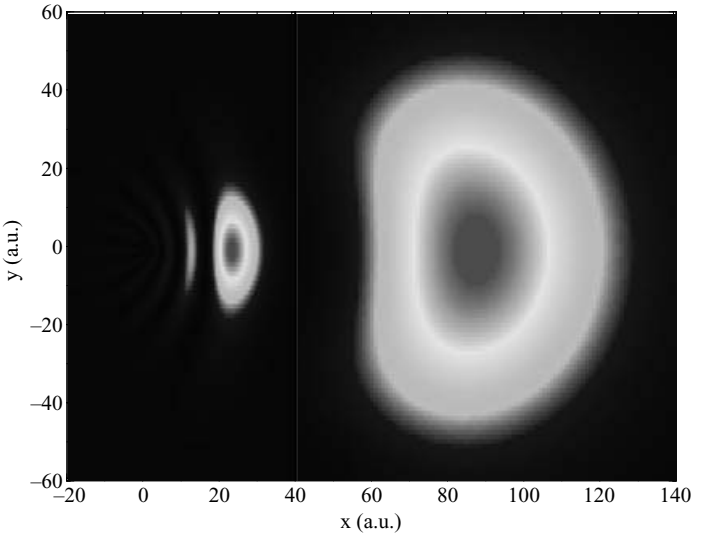

Fig. 10. Electronic density of the quantum mechanical ground state of the frozen planet configuration, in a two dimensional configuration space, for $N = 6$. The inner ($x \leqslant 40$ a.u.) and outer ($x \geqslant 40$ a.u.) electronic densities are plotted together in order to allow for an immediate comparison with the classical frozen planet orbit of Figure 9 (Madroñero and Buchleitner 2004).

idea of the reliability of such a restriction in view of the desired predictive power of theoretical results for realistic experimental scenarios, we have to gain some intuition for the localisation and decay properties of the unperturbed frozen planet.

Figures 9 and 10 compare a typical classical frozen planet trajectory with a small transverse excitation with the corresponding quantum mechanical electronic density in the plane. The one to one correspondence between the classical dynamics and the localisation properties of the quantum mechanical eigenfunction is apparent and unambiguous, and is basically due to the anchoring of the quantum eigenstate to the nonlinear resonance island

https://doi.org/10.1017/S0960129507005968 Published online by Cambridge University Press

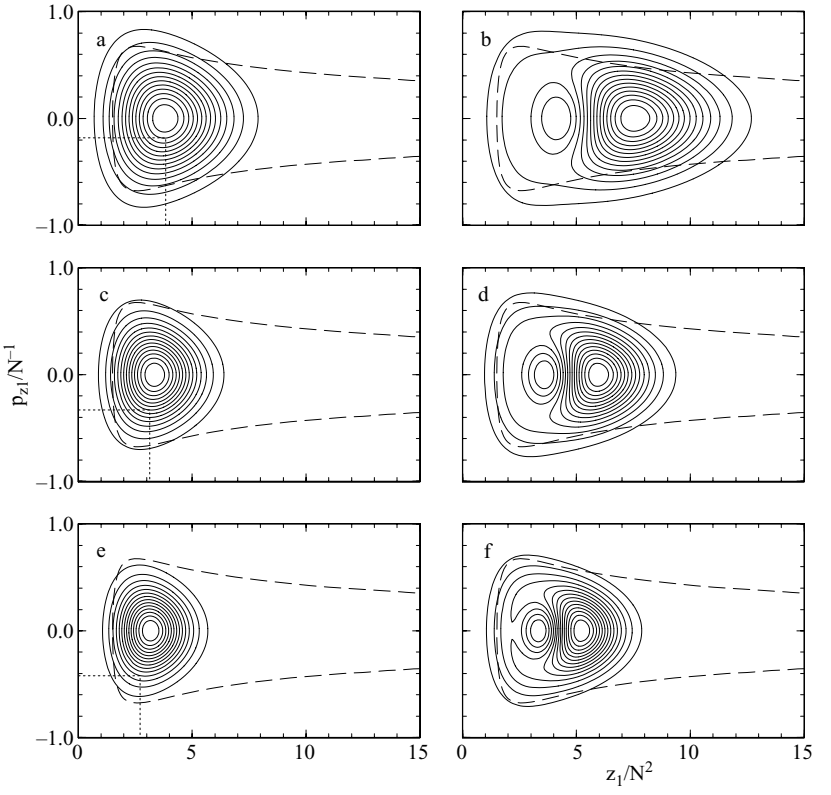

Fig. 11. Phase space projection (Husimi or Glauber-Q distribution) of the frozen planet ground (left) and first excited (right) state on the phase space of the outer electron, for different exctations $N = 3, 4, 5$ (from top to bottom) of the inner electron. Positions and momenta are rescaled as a function of the excitation N of the inner electron. The dashed line confines the resonance island that provides the classical anchoring place for the stable frozen planet configuration. The squares in the bottom left corners indicate the phase space volume occupied by the quantum unit of action, h, on the scale of the characteristic action of the classical frozen planet orbit.

that defines the frozen planet orbit in classical phase space (Holthaus 1995; Buchleitner *et al.* 2002): Figure 11 shows the phase space projection (by means of a Husimi or Glauber-Q quasiprobability distribution (Cohen-Tannoudji *et al.* 1992)) of the quantum mechanical ground state and of the first excited state of the frozen planet configuration, for increasing excitations N of the inner electron, that is, for increasing actions of the classical frozen planet orbit as compared to the quantum mechanical action unit h. The resulting improving resolution of classical phase space structures by the quantum phase space density is represented by the dotted squares in the lower left corner of the phase space plots. These indicate the effective phase space volume of h, on the scale of the characteristic action of the considered frozen planet orbit.

The dashed line in the figure confines the resonance island that defines the phase space volume of those trajectories that are bound by the effective frozen planet potential shown

https://doi.org/10.1017/S0960129507005968 Published online by Cambridge University Press

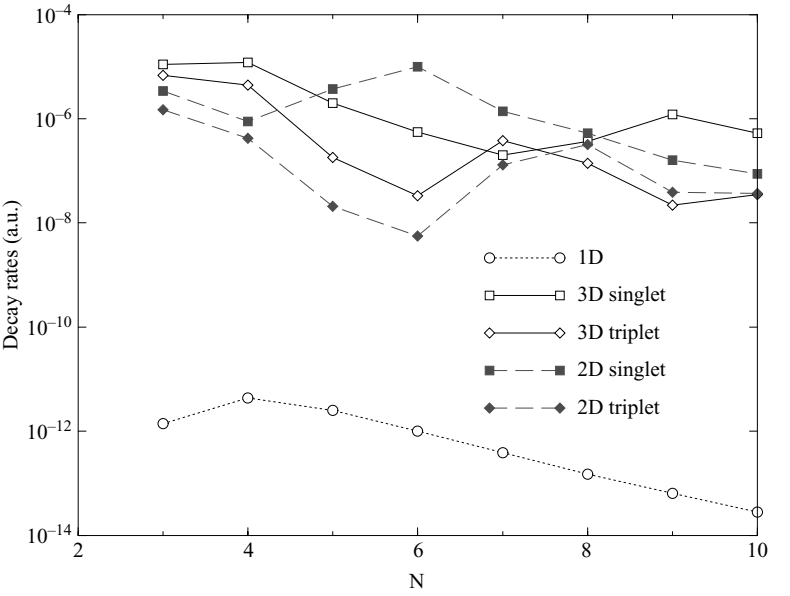

Fig. 12. Autoionisation rates of the unperturbed frozen planet configuration for one, two and three dimensions of configuration space, as a function of the inner electron's excitation N. The 1D result clearly shows that the autoionisation rates are exponentially suppressed once the quantum state is completely trapped by the underlying classical resonance island ($N \geqslant 4$, see Figure 11). Furthermore, the 2D and 3D results exhibit dramatically enhanced autoionisation rates compared with the 1D rates, and are additionally garnished with erratic fluctuations (due to chaos assisted tunnelling in the transverse phase space component (Schlagheck and Buchleitner 2003; Madroñero *et al.* 2005)). The comparatively small and unsystematic differences between 2D and 3D rates also suggest that a planar model of the real, 3D problem may even come up with quantitatively reliable predictions.

in Figure 7, and we clearly see that the frozen planet ground and excited states' projection fits better and better within this island as we increase the excitation (which is tantamount to decreasing the effective volume occupied by h). Correspondingly, the autoionisation rates are exponentially suppressed with N, once the frozen planet is completely trapped by the classical resonance island: this is quantified in Figure 12, for different dimensions of the accessible configuration space.

2.2.2. *Classical (in)stability under periodic driving* We will now take a closer look at the stability properties of the frozen planet configuration under periodic driving, which we have already briefly encountered in the middle and right-hand plots of Figure 8. These section surfaces spanned by the outer electron's momentum and position along the collinearity axis of the configuration, obviously represent only a *subspace* of the complete phase space – the latter, however, is hard to visualise by phase space sections, due to

https://doi.org/10.1017/S0960129507005968 Published online by Cambridge University Press

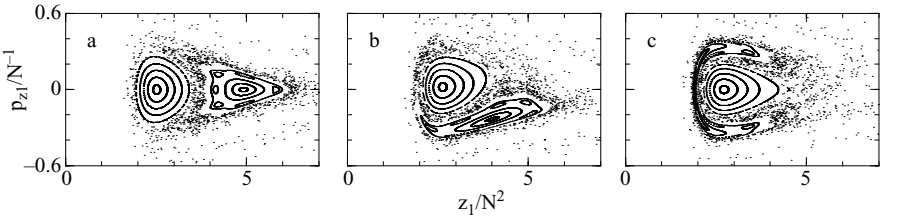

Fig. 13. Phase space (sub)structure of the outer electron of the driven frozen planet configuration, spanned by the electron's momentum and position in the collinear subspace. Positions and momenta are rescaled as a function of the excitation N of the inner electron. Due to the periodicity of the driving field, the phase space structure exhibits itself a periodic time dependence, here shown for phases $\omega t = 0$ (left), $\pi/2$ (middle), and π (right) of the driving field at frequency ω (Schlagheck and Buchleitner 2003).

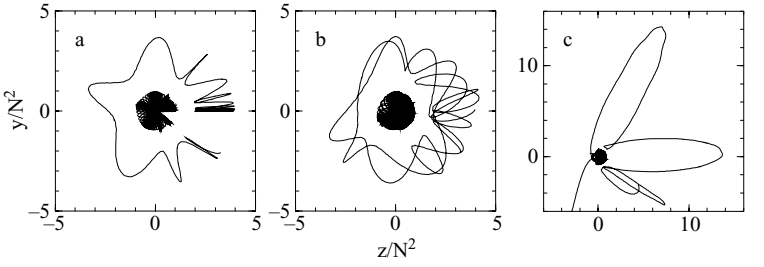

Fig. 14. Trajectory of the frozen planet configuration under external driving, in the full configuration space, from 0 to 15 (left), from 15 to 30 (middle) and from 75 to 91 (right) driving field periods. Positions and momenta are rescaled as a function of the excitation N of the inner electron. While the interelectronic correlation is still conserved for short times, it is destroyed at intermediate times, what finally leads to a collision of both electrons and subsequent (auto)ionisation of the configuration.

its high dimensionality†. To assess the stability properties of the driven configuration, we additionally have to monitor the dynamics for finite perturbations in the direction transverse to the collinearity axis. Indeed, while the driven dynamics in the collinear subspace exhibits completely regular dynamics within the driving-induced nonlinear resonance, see Figure 13, a transverse perturbation first destroys the correlation of the electronic dynamics and, consequently, then leads to the fragmentation of the configuration, as illustrated in Figure 14. By adding an additional, static electric field along the collinearity axis, we can suppress this instability: the static field confines the configuration within the vicinity of the collinearity axis, thus protecting it against decorrelation and subsequent fragmentation, as illustrated in Figure 15 (Schlagheck and Buchleitner 2003).

† As a matter of fact, plots like those in Figure 8 can only be obtained because of the separation of time scales between the inner and outer electron's characteristic frequencies; for details see Schlagheck and Buchleitner (1999).

https://doi.org/10.1017/S0960129507005968 Published online by Cambridge University Press

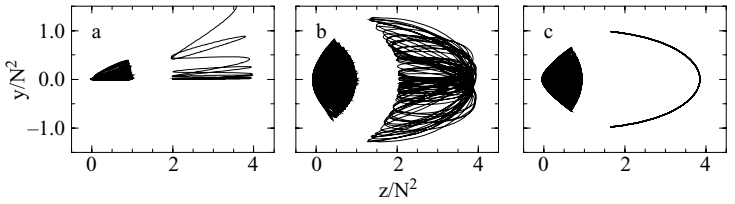

Fig. 15. Trajectory of the frozen planet configuration under external driving, in the full configuration space. Without a static field (a) the electrons perform chaotic rotations around the nucleus (as in Figure 14). An additional electrostatic field along the z-axis stabilises the trajectories, as shown in (b) and (c), for different initial conditions.

2.3. *Quantum dynamics of the driven frozen planet*

However, we are not really interested here in the classical dynamics of the driven frozen planet, but rather in its 'real' quantum dynamics. The above investigation of the classical motion only serves as a guideline for our subsequent quantum treatment, which, as we shall see, is not yet complete, though it has already given us some useful and encouraging insights.

2.3.1. *Technical ingredients* We will start from the beginning with a formal treatment of the quantum system to hand. The Hamiltonian of the driven helium atom is given, in atomic units, by

$$H = \frac{p_1^2 + p_2^2}{2m} - \frac{Z}{r_1} - \frac{Z}{r_2} + \frac{1}{r_{12}} + F(x_1 + x_2)\cos\omega t, \tag{2}$$

with the nuclear charge $Z = 2$, the reduced mass m of the electrons, cartesian positions $\mathbf{r_i}$ and momenta $\mathbf{p_i}$ of the electrons, interelectronic distance $r_{12} = |\mathbf{r_1} - \mathbf{r_2}|$, driving field amplitude F and frequency ω. The driving field is chosen to be linearly polarised along the $\hat{x}$ direction – thus the dipole coupling operator is given by $x_1 + x_2$. Configuration space is restricted to the plane containing all three interacting particles, together with the field vector of the driving field (Madroñero 2004).

In order to extract the full spectral structure that generates the atomic dynamics under the external perturbation, we merge several mathematical, theoretical and numerical tools. These are:

— *Floquet theory*, in order to account for the periodicity of the Hamiltonian (2). The Floquet theorem (Floquet, 1883; Shirley 1965; Ritus 1966; Zeldovich 1967) essentially derives time-periodic eigensolutions (with period $2\pi/\omega$) from the stationary eigenvalue problem

$$(H - i\partial_t)|\epsilon\rangle = \epsilon|\epsilon\rangle \tag{3}$$

on the space of square integrable, time periodic functions on configuration space, by considering time as an additional coordinate in an extended configuration (or phase) space (Lichtenberg and Lieberman 1983; Buchleitner *et al.* 2002). The periodic boundary conditions in time induce a periodicity of the eigenvalue spectrum with

https://doi.org/10.1017/S0960129507005968 Published online by Cambridge University Press

period ω on the energy axis, in complete analogy with the periodicity of the spectrum of a particle moving in a spatially periodic potential on the (quasi)momentum axis.

— *Complex rotation* (Balslev and Combes 1971; Reed and Simon 1990; Buchleitner *et al.* 1994) of the Floquet Hamiltonian $(H - i\partial_t)$, in order to assess the eigenenergies together with the associated (auto)ionisation rates of the atomic eigenstates in the driving field ('dressed states' in quantum optical jargon, or 'Floquet states' as their semiclassical counterparts, where 'semiclasscial' refers to the classical (rather than quantised) description of the field degree of freedom in (2)). This amounts to a non-unitary transformation of the Hamiltonian, essentially by complexifying position and momentum,

$$\mathbf{x} \to \mathbf{x}\exp(i\theta), \quad \mathbf{p} \to \mathbf{p}\exp(-i\theta)\,, \tag{4}$$

leaving us with a *complex symmetric* rather than hermitian eigenvalue problem. The complex eigenvalues obtained by diagonalisation of the complex rotated Floquet Hamiltonian are just the poles of the resolvent of $H - i\partial_t$, in the lower half of the complex plane, with real parts giving the energies of the associated (auto)ionising resonance states, and imaginary parts giving half the (auto)ionisation rates Γ, that is,

$$\mathrm{Re}(\epsilon) = E\,,\ \mathrm{Im}(\epsilon) = -\Gamma/2\,. \tag{5}$$

In addition, the diagonalisation (necessarily in a finite basis) also yields the discretised continuum states, which are rotated into the lower half of the complex plane by an angle 2θ, with θ the real-valued complex rotation parameter in (4). Complex rotation thus separates the structured resonance part from the flat background of the strictly continuous spectrum of the driven atom.

— *A two-fold parabolic coordinate transformation, amended by a rotation* (Hilico *et al.* 2002; Madroñero 2004), which allows us to rewrite (2) as a closed polynomial in the creation and annihilation operators $a_i^\dagger, a_i$, $i = 1, \ldots, 4$, of four (coupled) harmonic oscillators. The resulting expression for the complete Hamiltonian, including the time dependent drive, is too lengthy to be presented here (it has 5742 terms), but even the polynomial representation of the *unperturbed* helium Hamiltonian (that is, for vanishing field amplitude), which has the 423 terms shown in Figure 16, already suggests the dramatic complexity brought about by the interelectronic repulsion when compared with the simple one electron Coulomb problem.

— *Advanced parallel programming* (Madroñero and Buchleitner 2004) on some of the largest parallel supercomputing architectures to handle the typical size of the (generalised) complex symmetric eigenvalue problem that needs to be solved: memory requests range from approximately 500 GB to a little less than 700 GB, for excitations up to $N = 6$ of the inner electron, and driving frequencies that are near resonant with the fundamental frozen planet trajectory.

2.3.2. *Nondispersive two-electron wave packets* Using this machinery, we obtain typical complex eigenvalue spectra as displayed in Figures 17 and 18 for, respectively, the field-free and periodically driven helium atom in the doubly excited spectral range. The unperturbed helium spectrum, Figure 17, clearly exhibits the accumulation points of the single electron

https://doi.org/10.1017/S0960129507005968 Published online by Cambridge University Press

Fig. 16. Polynomial representation of the unperturbed helium Hamiltonian in the plane, in the creation and annihilation operators of four coupled harmonic oscillators. The expression has 423 terms, and can be evaluated analytically in the associated oscillator basis. The polynomial is of maximal degree 12 for the unperturbed problem. In the presence of an oscillating external field, the order increases to 16 (Madroñero 2004).

https://doi.org/10.1017/S0960129507005968 Published online by Cambridge University Press

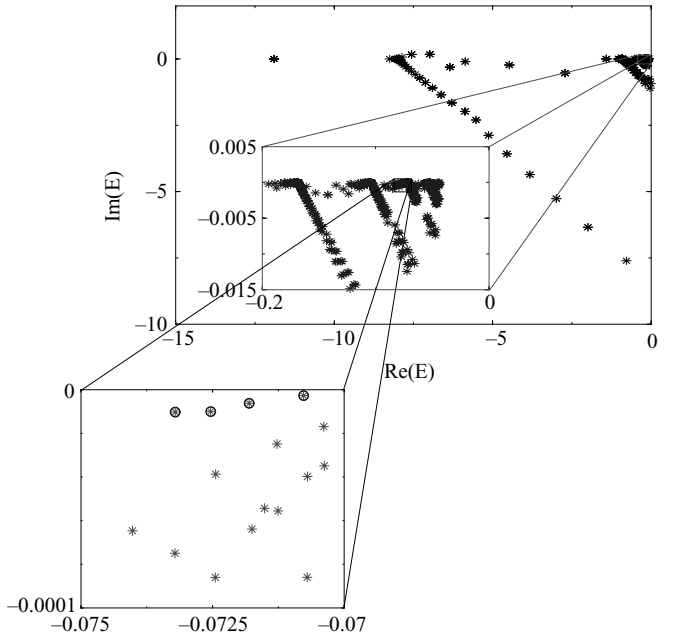

Fig. 17. Complex eigenvalue spectrum of the complex rotated Hamiltonian of the unperturbed helium atom. Single ionisation thesholds converging towards the double ionisation threshold are clearly identified (first zoom), as well as the discretised continua, which appear as straight lines in the lower complex plane, under a finite angle with respect to the real energy axis. The fundamental and excited frozen planet states are easily identified by (a) their localisation properties, quantified by the expectation value $\langle \cos \theta_{12} \rangle$ of the interelectronic angle θ_{12}, and (b) their extremely long life times, often actually the longest life times observed within a given spectral interval (circled states in the second zoom).

Rydberg series on the real axis, which themselves converge towards the double ionisation threshold, as evident from the first inset zooming into the high energy domain. Also, the rotated discretised continua are easily distinguishable. The second inset zooms even deeper into the spectrum close to the $N = 6$ single ionisation channel in order to allow for the identification of the frozen planet states of the $N = 6$ series. Indeed, with the additional criterium that the interelectronic angle θ_{12} (with respect to the fixed nucleus) vanishes, that is, $\langle \cos \theta_{1,2} \rangle \simeq 1$, which can be evaluated on the eigenvectors obtained from the diagonalisation, the frozen planet states are easily found even at high spectral densities. As a matter of fact, they also have the characteristic signature of exhibiting the longest life times in the spectral range under consideration – which is an immediate expression of the trapping of the quantum mechanical eigenstates by the nonlinear resonance in classical phase space, which we have already observed in Figures 11 and 12.

The spectral structure becomes considerably more complicated in the presence of the external drive, as is immediately apparent from Figure 18: the driving field couples different angular momenta, and the density of states increases dramatically. Finding specific eigenstates now becomes a much more complicated endeavour, similar to the

https://doi.org/10.1017/S0960129507005968 Published online by Cambridge University Press

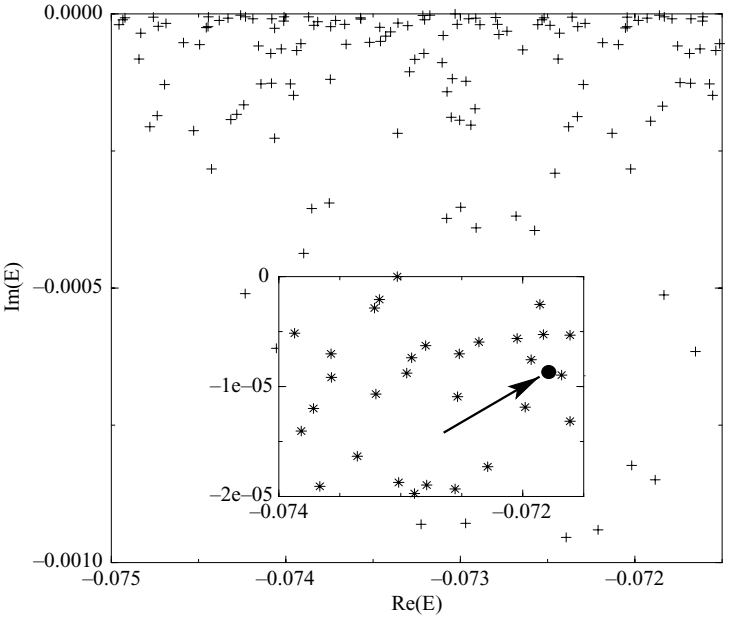

Fig. 18. Complex eigenvalue spectrum of the complex dilated Floquet Hamiltonian. The characteristic periodicity of the spectrum with the driving field frequency ω is apparent, while the single electron Rydberg series converging towards the double ionisation threshold in Figure 17 completely disappeared, as a consequence of the field-induced multiphoton coupling of different series. The arrow in the inset indicates the resonance which represents the eigenstate projected on classical phase space in Figure 19.

search for a needle in a haystack. Yet, once again by classifying the obtained eigenvectors according to their decay rates and the relative localisation properties of the two electrons, it is possible to single out eigenstates with particularly attractive properties. One such eigenstate is represented in Figure 19, by its Husimi quasiprobability on the phase space of the outer electron's collinear subspace. It is immediately apparent from a comparison of the state's phase space dynamics with the underlying classical phase space structure that it is anchored to the nonlinear classical resonance island induced by the near resonant driving of the frozen planet by the external field. Since the eigenstate is a Floquet state, its dynamics is, by construction, periodic in time. Thus, the wave packet does not disperse (dispersion is inhibited by the classical resonance island), despite the fact that the driven helium atom is a manifestly unharmonic system (Schrödinger 1926; Buchleitner *et al.* 2002). Rather, it is localised on the resonantly driven frozen planet trajectory, and performs quasiclassical motion along this trajectory (in much the same way as with the nonlinear resonance island). In principle, the Floquet theorem tells us that this dynamics would continue forever if it were not for the nonvanishing coupling (mediated by the electron–electron interaction as well as by field induced multiphoton transitions) to single or double ionisation continua. In the semiclassical picture suggested by our comparison of classical and quantum dynamics in Figure 19, this coupling is

https://doi.org/10.1017/S0960129507005968 Published online by Cambridge University Press

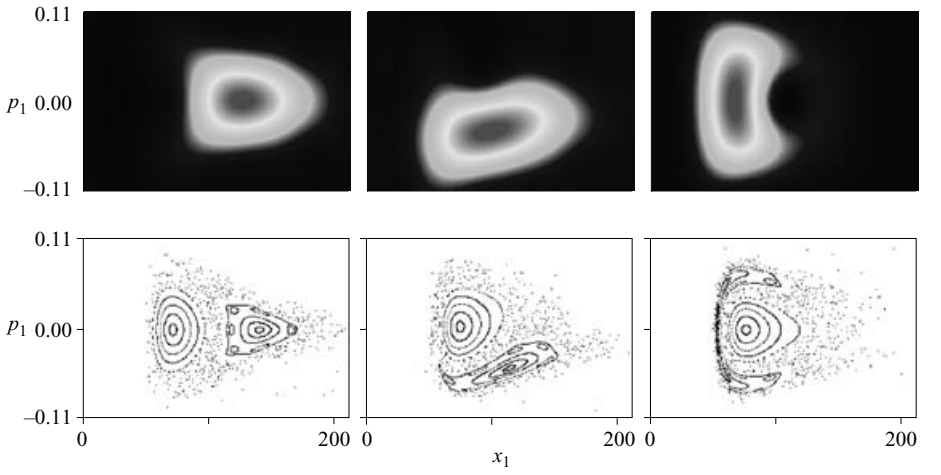

Fig. 19. Top: Husimi or Glauber-Q quasiprobability of the eigenstate associated with the complex eigenvalue highlighted by the arrow in the inset of Figure 18, for different phases $\omega t = 0$ (left), $\pi/2$ (middle), and π (right) of the driving field. The dynamics of the wave function is compared to the time evolution of the classical phase space structure in the bottom row. The quantum state is unambiguously localised on top of the classical nonlinear resonance island induced by resonant driving of the frozen planet trajectory by the external field. Its nondispersive evolution along the frozen planet trajectory qualifies the state as a nondispersive two-electron wave packet.

tantamount to a nonvanishing tunnelling probability from the inside to the outside of the field induced resonance island, and indeed gives rise to typical life times (inverse decay rates) of approximately $700 \ldots 1000 \times 2\pi/\omega$. This finite life time of the quasiclassical two-electron wave packet is long with respect to life times of most Rydberg wave packets so far produced in the lab (Raman *et al.* 1997), though short when compared with the life times of the one electron nondispersive Rydberg wave packets predicted (Buchleitner and Delande 1995) and observed (Maeda and Gallagher 2004; Maeda *et al.* 2005) for resonantly driven hydrogen like species. Once again, as already observed in Figure 12, the life time will increase with increasing excitation in the doubly excited Rydberg range, but numerical resources currently limit us to excitations that are no higher than the $N = 6$ channel.

Finally, we should stress that the nondispersive wave packets that we predict here are particularly robust against uncontrolled perturbations (ubiquitous in any real world laboratory), as a consequence of the Kolmogorov–Arnold–Moser theorem (Lichtenberg and Lieberman 1983): small perturbations, due to, for example, stray electric fields, will leave the topology of the nonlinear resonance island in phase space essentially unaffected – the island may get squeezed or deformed like a cushion, yet it will survive as a phase space structure lending support to a nondispersive wave packet eigenstate. Thus, one of the fundamental theorems of the mathematical theory of nonlinear Hamiltonian dynamics has an immediate and *highly relevant* bearing on laboratory experiments. Therefore, nondispersive wave packets anchored to nonlinear resonance islands in classical

https://doi.org/10.1017/S0960129507005968 Published online by Cambridge University Press

phase space open completely novel perspectives for coherent quantum control, with unprecedented robustness against uncontrolled experimental noise (Maeda and Gallagher 2004).

3. Conclusion

We have given some evidence that the driven three body Coulomb problem forms a formidable challenge for quantum theory in general, and for computational atomic physics in particular. As a first result, we have isolated non-dispersive two electron wave packets within the complex energy spectrum as a hall-mark of nonlinear resonance islands in classical phase space and of the Kolmogorov–Arnold–Moser theorem, as far as their robustness against perturbations is concerned. We have seen that in the quest for predictive power we have had to employ the largest computational recources available (combined with a considerable effort in efficient parallel programming), and that even more powerful resources will be needed for a faithful description of the fully fledged 3D problem in the presence of an external drive. On the other hand, without the (semi)classical intuition gained from simulations of the classical dynamics, it would be very hard to identify frozen planet states and nondispersive wave packets in the apparently unstructured, densly packed quantum spectrum, let alone to understand their surprisingly long life times, as well as their robustness. Furthermore, semiclassical considerations identify the arithmetic backbone of the quantum spectrum, and, in particular, the nonlinear resonance island to which the wave packets are anchored through the resonance condition $m\Omega = \omega$ between the external drive and the unperturbed frozen planet frequency. Thus, they help to identify the fingerprints of discrete arithmetic structures in a quantum system with a strictly continuous spectrum.

Acknowledgements

We acknowledge partial financial support by the DAAD, within the PROCOPE program.

Andreas Buchleitner acknowledges the support of the European Community under the Marie Curie Host Fellowships for the Transfer of Knowledge during his visit to Universytet Jagielloński, and, in particular, the hospitality of Jakub Zakrzewski's and Karol Życzkowski's research groups there.

References

Balslev, E. and Combes, J. M. (1971) Spectral properties of many-body Schrödinger operators with dilation-analytic interactions. *Commun. math. Phys.* **22** 280.

Bohigas, O. (1991) Random matrix theories and chaotic dynamics. In: *Chaos and quantum physics*, Les Houches Lectures, North-Holland 87.

Bohr, N. (1936) *Nature* **137** 344.

Buchleitner, A. and Delande, D. (1995) Nondispersive electronic wave packets in multiphoton processes. *Phys. Rev. Lett.* **75** 1487.

Buchleitner, A., Delande, D. and Zakrzewski, J. (2002) Non-dispersive wave packets in periodically driven quantum systems. *Phys. Rep.* **368** 409.

Buchleitner, A., Grémaud, B. and Delande, D. (1994) Wave functions of atomic resonances. *J. Phys. B: Atom. Mol. Opt. Phys.* **27** 2663.

Chirikov, B. V. (1959) The passage of a nonlinear oscillating system through resonance. *Sov. Phys. Dokl.* **4** 390.

Cohen-Tannoudji, C., Dupont-Roc, J. and Grynberg, G. (1992) *Atom-Photon Interactions*, John Wiley and Sons Inc.

Corkum, P. (1993) Plasma perspective on strong field multiphoton ionization. *Phys. Rev. Lett.* **71** 1994.

Einstein, A. (1917) Zum Quantensatz von Sommerfeld und Epstein. *Verh. Dtsch. Phys. Ges.* **19** 82.

Esra, G., Richter, K., Tanner, G. and Wintgen, D. (1991) Semiclassical cycle expansion for the helium atom. *J. Phys. B* **24** L413.

Floquet, M. G. (1883) Équations différentielles linéaires à coefficients périodiques. *Annales de l'École Normale Supérieure* **12** 47.

Greiner, M., Mandel, O., Esslinger, T., W.Hänsch, T. and Bloch, I. (2002) Quantum phase transition from a superfluid to a Mott insulator in a gas of ultracold atoms. *Nature* **415** 39.

Hilico, L., Grémaud, B., Jonckheere, T., Billy, N. and Delande, D. (2002) Quantum three-body Coulomb problem in two dimensions. *Phys. Rev. A* **66** 22101.

Holthaus, M. (1995) On the classical-quantum correspondence for periodically time dependent systems. *Chaos, Solitons and Fractals* **5** 1143.

Kramer, B. and MacKinnon, A. (1993) Localization: Theory and experiment. *Rep. Prog. Phys.* **56** 1469.

Lappas, D. G., Sanpera, A., Watson, J. B., Burnett, K. and Knight, P. L. (1996) Two-electron effects in harmonic generation and ionization from a model He atom. *J. Phys. B: Atom. Mol. Opt. Phys.* **29** L619.

Lein, M., Gross, E. and Engel, V. (2000) Intense-field double ionization of helium: Identifying the mechanism. *Phys. Rev. Lett.* **85** 4707.

Lichtenberg, A. J. and Lieberman, M. A. (1983) *Regular and Stochastic Motion*, Applied Mathematical Sciences **38**, Springer-Verlag.

Madroñero, J. (2004) *Spectral structure of planar helium under periodic driving*, Ph.D. thesis, Ludwig-Maximilians-Universität München. (Available at `http://edoc.ub.uni-muenchen.de/archive/00002187/`.)

Madroñero, J. and Buchleitner, A. (2004) Planar helium under electromagnetic driving. In: *High Performance Computing in Science and Engineering, Munich 2004 – Transactions of the Second Joint HLRB and KONWIHR Result and Reviewing Workshop, March 2nd and 3rd, 2004, Technical University of Munich*, Springer-Verlag.

Madroñero, J., Schlagheck, P., Hilico, L., Grémaud, B., Delande, D. and Buchleitner, A. (2005) Decay rates of planar helium. *Europhys. Lett.* **70** 183.

Maeda, H. and Gallagher, T. (2004) Nondispersing wave packets. *Phys. Rev. Lett.* **92** 133004.

Maeda, H., Norum, D. and Gallagher, T. F. (2005) Microwave manipulation of an atomic electron in a classical orbit. *Science* **307** 1757.

Nikolopoulos, L. and Lambropoulos, P. (2001) Multichannel theory of two-photon single and double ionization of helium. *J. Phys. B: Atom. Mol. Opt. Phys.* **34** 545.

Ostrovsky, V. N. and Prudov, N. V. (1995) Adiabatic theory for the doubly excited asymmetric states of the helium atom. *Phys. Rev.* **A51** 1936.

Parker, J. S., Moore, L. R., Dundas, D. and Taylor, K. T. (2000) Double ionization of helium at 390 nm. *J. Phys. B* **33** L691.

Raman, C., Weihnacht, T. and Bucksbaum, P. (1997) Stark wave packets viewed with half-cycle pulses. *Phys. Rev. A* **55** R3995.

Reed, M. and Simon, B. (1990) *Analysis of Operators, Methods of Modern Mathematical Physics*, Academic Press.

Richter, K., Tanner, G. and Wintgen, D. (1993) Classical mechanics of two-electron atoms. *Phys. Rev.* **A48** 4182.

Richter, K. and Wintgen, D. (1990) Stable planetary atom configurations. *Phys. Rev. Lett.* **65** 1965.

Ritus, V. I. (1966) Shift and splitting of atomic levels caused by the field of an electromagnetic wave. *Zh. Eksp. Teor. Fiz.* **51** 1492.

Ruiz, C., Plaja, L., Roso, L. and Becker, A. (2006) Ab initio calculation of the double ionization of helium in a few-cycle laser pulse beyond the one-dimensional approximation. *Phys. Rev. Lett.* **96** 053001.

Russell, B. (1970) *Das ABC der Relativitätstheorie*, Fischer Verlag.

Schlagheck, P. and Buchleitner, A. (1999) Stable configurations in the strongly driven helium atom. *Physica D* **131** 110.

Schlagheck, P. and Buchleitner, A. (2003) Nondispersive two-electron wavepackets in driven helium. *Eur. Phys. J. D* **22** 401.

Schrödinger, E. (1926) Der stetige Übergang von der Mikro- zur Makromechanik. *Die Naturwissenschaften* **14** 664.

Scrinzi, A. and Piraux, B. (1997) Ionization and double excitation of helium by short intense laser pulses. *Phys. Rev. A* **56** R13.

Shirley, J. H. (1965) Solution of the Schrödinger equation with a Hamiltonian periodic in time. *Phys. Rev.* **138** B979.

Störzer, M., Gross, P., Aegerter, C. M. and Maret, G. (2006) Observation of the critical regime near Anderson localization of light. *Phys. Rev. Lett.* **96** 063904.

Tanner, G., Richter, K. and Rost, J. (2000) The theory of two-electron atoms: between ground state and complete fragmentation. *Rev. Mod. Phys.* **72** 497.

von Brentano, P., Ernst, J., Hausser, O., Mayer-Kuckuk, T., Richter, A. and von Witsch, W. (1964) Statistical fluctuations in the cross sections of the reactions Cl-35 (p,alpha) S-32 and Cl-37 (p,alpha) S-34. *Phys. Lett.* **9** 48.

Walker, B., Sheehy, B., DiMauro, L. F., Agostini, P., Schafer, K. J. and Kulander, K. C. (1994) Precision measurement of strong field double ionization of helium. *Phys. Rev. Lett.* **73** 1227.

Wellens, T., Grémaud, B., Delande, D. and Miniatura, C. (2005) Coherent backscattering of light by nonlinear scatterers. *Phys. Rev. A* **71** 55603.

Wigner, E. (1959) *Group Theory and its Application to the Quantum Mechanics*, Academic Press.

Zeldovich, Y. B. (1967) The quasienergy of a quantum-mechanical system subjected to a periodic action. *JETP (Soviet Physics)* **24** 1006.